polymers

MDPI

Review

Recent Advances in the Removal of Organic Dyes from Aqueous Media with Conducting Polymers, Polyaniline and Polypyrrole, and Their Composites

Jaroslav Stejskal

University Institute, Tomas Bata University in Zlin, 760 01 Zlin, Czech Republic; stejskal@utb.cz

Abstract: Water pollution by organic dyes, and its remediation, is an important environmental issue associated with ever-increasing scientific interest. Conducting polymers have recently come to the forefront as advanced agents for removing dye. The present review reports on the progress represented by the literature published in 2020–2022 on the application of conducting polymers and their composites in the removal of dyes from aqueous media. Two composites, incorporating the most important polymers, polyaniline, and polypyrrole, have been used as efficient dye adsorbents or photocatalysts of dye decomposition. The recent application trends are outlined, and future uses also exploiting the electrical and electrochemical properties of conducting polymers are offered.

Keywords: conducting polymers; composites; organic dyes; dye adsorption; dye removal; photocatalytic decomposition; polyaniline; polypyrrole

Citation: Stejskal, J. Recent Advances in the Removal of Organic Dyes from Aqueous Media with Conducting Polymers, Polyaniline and Polypyrrole, and Their Composites. *Polymers* **2022**, *14*, 4243. https://doi.org/10.3390/polym14194243

Academic Editor: George Z. Kyzas

Received: 7 September 2022
Accepted: 4 October 2022
Published: 10 October 2022

1. Introduction

The removal of water-soluble organic dyes from aqueous media using composites based on conducting polymers has recently been reviewed [1]. The present article updates this research direction's progress made in the last three years, 2020–2022. It is aimed at the organization of the recent studies by their objects of investigation rather than the compilation of experimental results. These are difficult to compare due to the widely differing experimental conditions, viz., the composition and concentration of adsorbents or photocatalysts, and the content of dye sorbates. Other reviews have recently been published on this topic and offer supplementary or alternative views [2–4].

Conducting polymers, such as polyaniline and polypyrrole (Scheme 1) and also, exceptionally, their substituted derivatives, have become an under consideration in the environmental sciences for water-pollution treatment. In principle, they can be used alone as powders. More often, however, they are applied as simple binary composites comprising an inorganic component, which provides some value-added, e.g., magnetic or photocatalytic properties. Alternatively, the composite component may be a natural or synthetic polymer affording the mechanical and material properties required by the applications, e.g., in the preparation of membranes or sponges. Finally, typical ternary composites include both inorganic and organic components, in addition to the conducting polymers.

The remediation of wastewater polluted by organic dyes is an important environmental goal. Conducting polymers are insoluble in aqueous media. When added to a solution of an organic dye, the reduction in the optical absorption reflecting the decreasing dye concentration has often been reported [1]. The process is classified as dye removal from the point of view of ecology (Scheme 1). Its mechanism is based on dye adsorption or its photocatalytic decomposition, or both occur simultaneously or in succession in various proportions.

Polyaniline [5] (Figure 1), probably the most common conducting polymer, is typically prepared by the oxidation of aniline in an acidic aqueous medium with ammonium peroxydisulfate [6]. The polymerization starts with common chemicals and proceeds easily at

room temperature, in the open air, within tens of minutes, and at a stoichiometric yield. The conducting polyaniline salt (Figure 1) has an electronic conductivity in the units of S cm^{-1}. The ease of preparation at an economic cost makes polyaniline an attractive object of application. Its hydrophilic, thin films have an emerald-green color. Under alkaline conditions, polyaniline salt converts to a nearly hydrophobic non-conducting blue base; the transition occurs at pH 4–6. For that reason, the interaction with organic dyes will be pH-dependent. On the other hand, most of the studies refer to the neutral conditions met in practice.

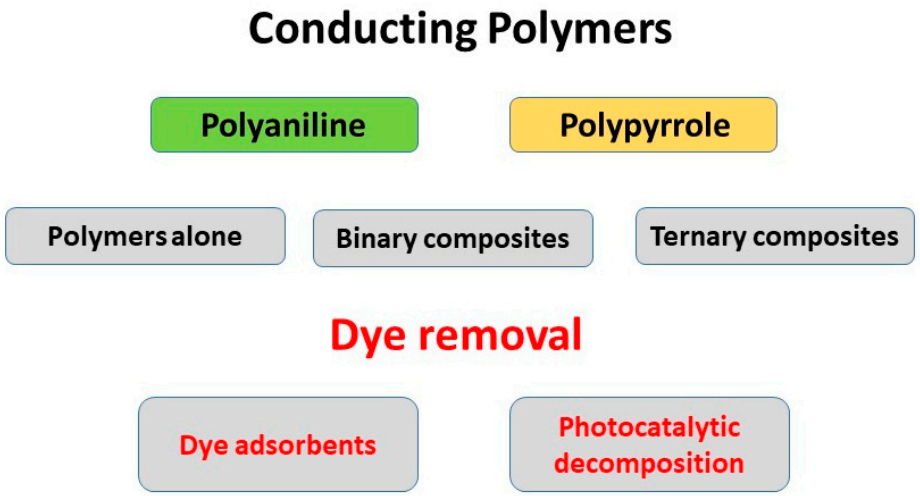

Scheme 1. Conducting polymers, polyaniline, or polypyrrole, have recently been used alone or in the composites for organic dye removal from aqueous media by adsorption or photocatalytic decomposition.

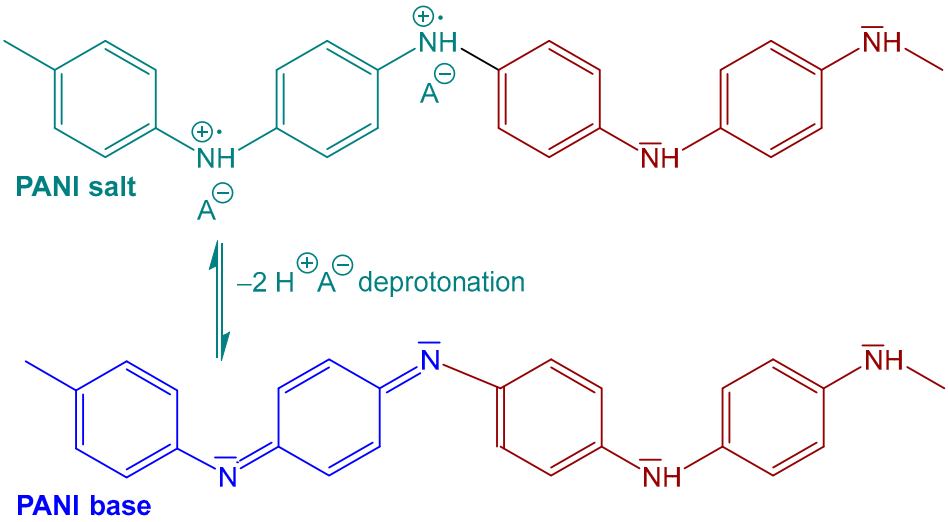

Figure 1. Polyaniline salt and base. A^- is a counter-ion, usually chloride or sulfate.

Conducting polymers, and many organic dyes, illustrated on polyaniline and methyl orange (Figure 2), share a similar molecular structure. They have a system of conjugated single and double bonds that are responsible for their color. They typically contain aromatic benzenoid or quinonoid rings. Nitrogen atoms, in their structure, are able to be hydrogen bonded. In addition to the hydrophobic organic section, the dyes include a charged ionic group that affords solubility in water. The same applies to the conducting polymers, which, however, are insoluble in water due to extensive intermolecular hydrogen bonding.

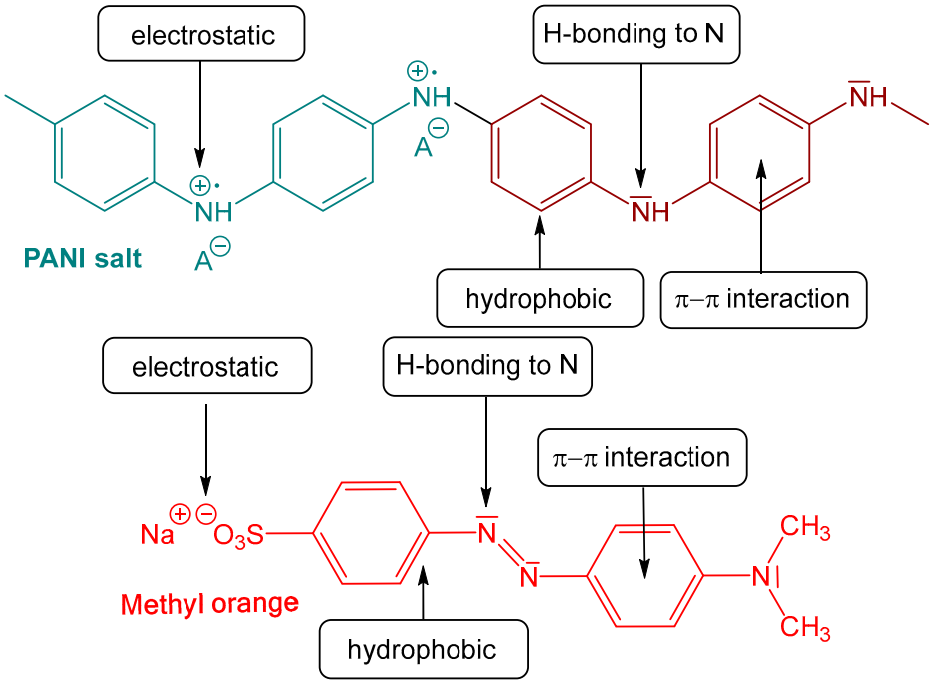

Figure 2. A conducting polymer, polyaniline, and an organic dye, methyl orange, and sites of their possible interactions.

Many organic dyes are used as acidobasic indicators. For example, the yellow color of methyl orange changes under neutral pH conditions to red when acid is added, with the transition range being pH 3.1–4.4 (Figure 3). However, not only does the color change but the molecular structure and hydrophobicity are also altered simultaneously; while the salt is well soluble, the acid form is not. This means that the interactions between polyaniline and methyl orange will occur between different species under different pH. This fact should be kept in mind. Methyl orange is also one of the common azo dyes extensively used in textile, paper, printing, and food industries and often contaminates industrial wastewater.

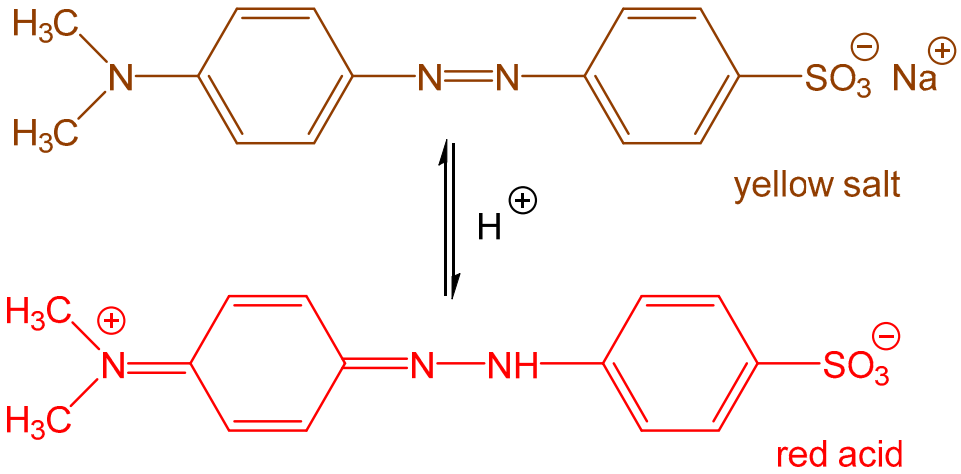

Figure 3. Yellow methyl orange salt converts to red acid under acidic conditions.

The interactions between the organic dyes and conducting polymers are responsible for the dye removal from aqueous media [1,7]. The *adsorption* of dyes on conducting polymers has often been reasonably proposed as the most relevant possibility. Adsorption is a surface phenomenon that occurs when the dye is expected to be attached to the conducting polymer surface by physical van der Waals forces or due to physicochemical interactions, e.g., of the

π–π electron type. Conducting polymers have a typical specific area of tens m^2g^{-1} [8], far lower than classical adsorbents when this parameter is one or two orders of magnitude higher. The adsorption, thus, probably cannot be the exclusive mechanism of efficient dye removal. The dye *absorption* is thus likely to occur after the dye molecules diffuse into the conducting polymer phase, a process much slower compared with the adsorption. Conducting forms of polyaniline and polypyrrole are hydrophilic and penetrable with an aqueous phase.

There is a choice of attractive interactions that occur, both during the adsorption or absorption. One possibility is the *π–π interaction* between the aromatic rings present in typical dyes and conducting polymers. The *electrostatic interactions*, when a soluble anionic dye produces insoluble salt with the conducting polymers, also need to be considered. The *hydrogen bonding* of hydrogen atoms in conducting polymers to nitrogen atoms in dyes or vice versa is probably one of the strongest interactions to account for. Finally, the *hydrophobic interactions*, when the non-ionic parts of conducting polymers (Figure 1) and dyes prefer to contact each other instead of with water, are analogous to the formation of surfactant micelles. Indeed, water-soluble dye molecules composed of a hydrophobic body and ionic group conform to the definition of surfactants.

The *photocatalytic decomposition* of dyes has also often been reported in the literature. In this case, the dye is removed by the degradation process to colorless products with the help of photogenerated active peroxide species. Such a mechanism is relevant when the dye removal occurring in the dark and when exposed to illumination considerably differ, the latter being faster [9]. Synergistic dye adsorption is usually also operational in these experiments [10]. The fact that the conducting polymers are colored, i.e., they efficiently absorb the visible light, which may hinder the light penetration to the photocatalyst interior, has not been discussed.

Polypyrrole is another conducting polymer (Figure 4). Its common globular form has a conductivity comparable to polyaniline, the units of S cm^{-1}. The transition between the conducting salt and the less conducting base is shifted to a much lower pH [11]. The adsorption is thus likely to depend on the pH [12]. Under neutral pHs, most often met in practice, polypyrrole maintains its conducting form, whereas polyaniline may start to lose its conductivity due to deprotonation (Figure 1).

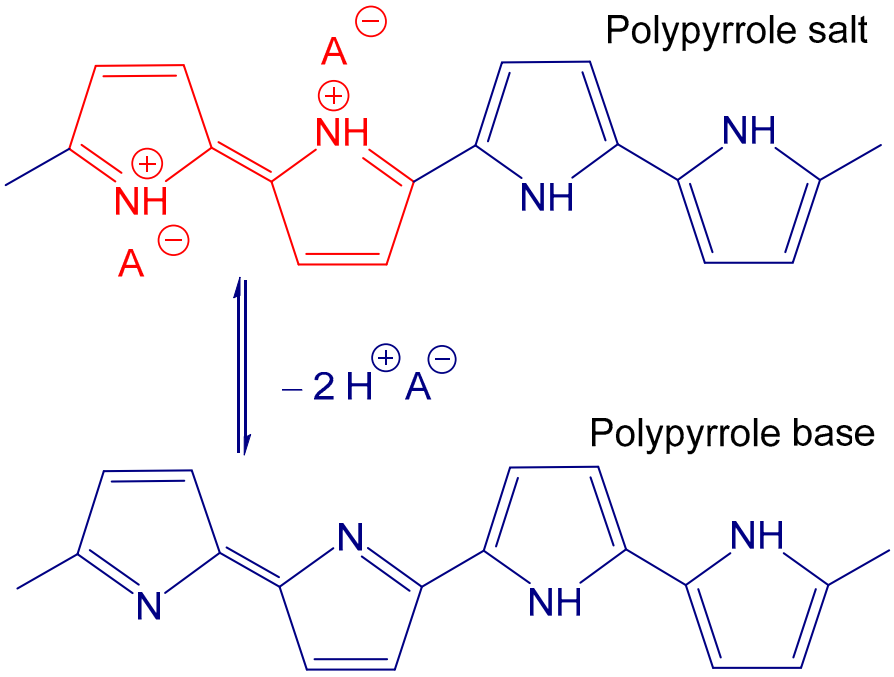

Figure 4. Polypyrrole salt and base. A^- is a counter-ion, usually chloride or sulfate.

Polyaniline and polypyrrole have a typical globular morphology (Figure 5). In contrast to polyaniline, polypyrrole converts its morphology from a globular to a nanotubular state (Figure 5) when its preparation occurs in the presence of methyl orange dye. At the same time, the conductivity of polypyrrole increases by one order of magnitude to tens S cm^{-1} [13]. The morphology and conductivity of polypyrrole may be controlled by introducing various dyes, again in contrast to polyaniline [14]. Especially in the case of polypyrrole, it is important to distinguish between the globular and nanotubular forms that behave differently with respect to the dye removal [15,16].

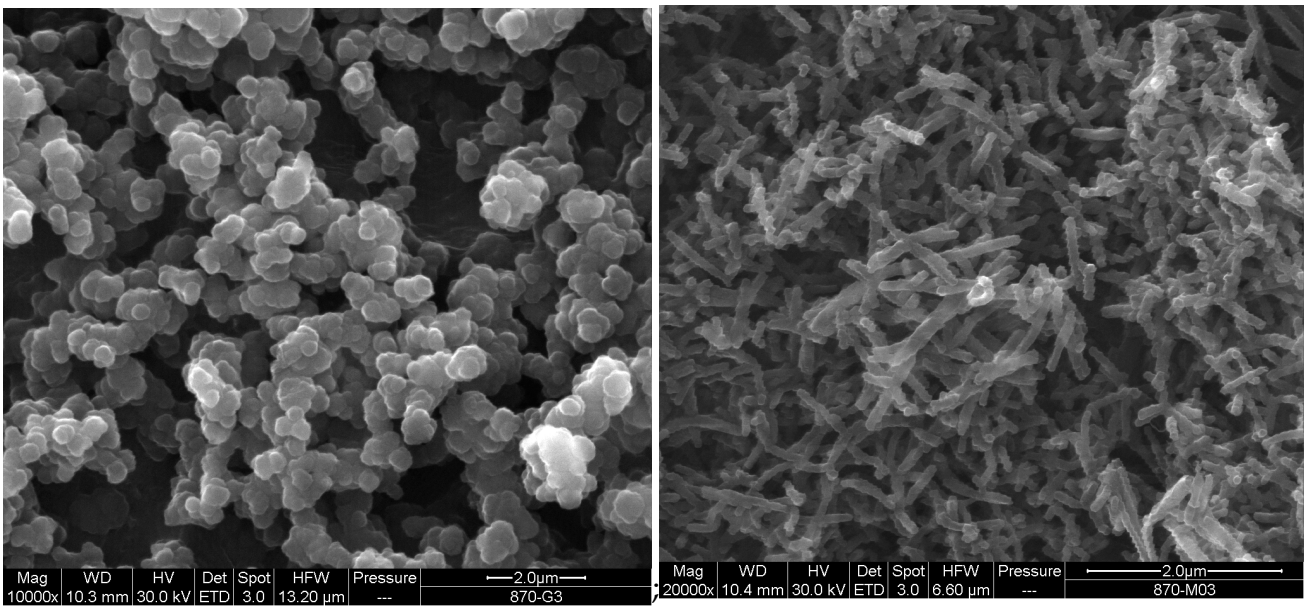

Figure 5. Globular polypyrrole (**a**) and polypyrrole nanotubes (**b**).

Another reason for the numerous studies reporting dye removal (Figure 6) [17,18] is the ease of the experimental procedure based on the UV-visible spectroscopy that monitors the optical absorption of dye solution in time after the addition of a conducting polymer or its composite (Figure 7). Such removal experiments have been carried out under static conditions and only exceptionally in a dynamic mode [19]. The most often used dyes used in the experiments are methyl orange, Congo red, methylene blue, and Rhodamine B (Figure 8).

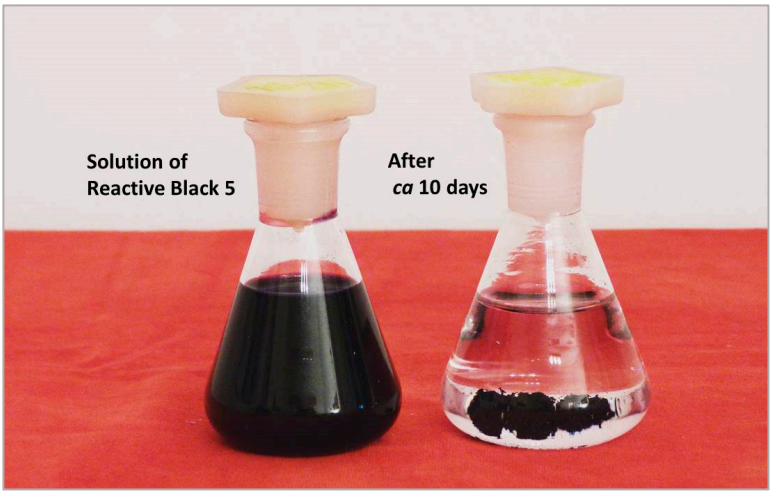

Figure 6. The solution of Reactive Black 5 before (**left**) and after dye adsorption by polypyrrole nanofibers (**right**). Adapted from [16].

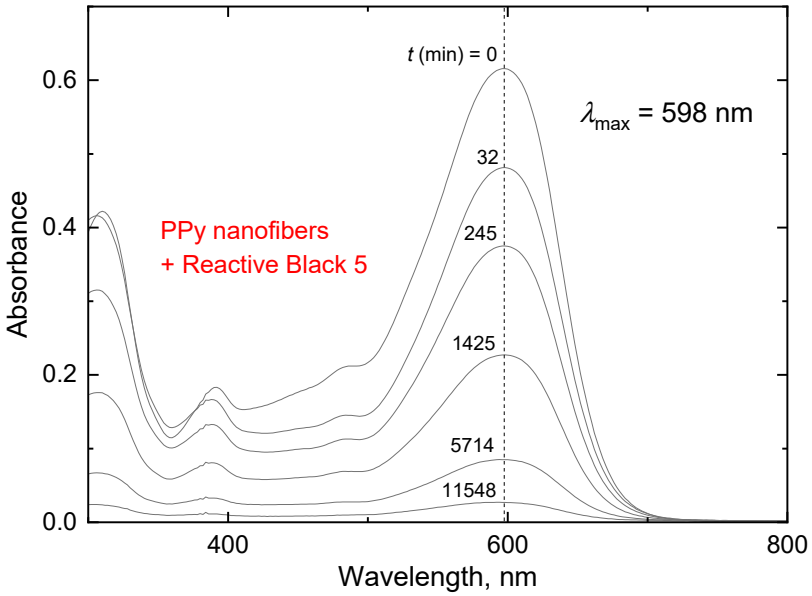

Figure 7. The decrease in the optical absorbance of the Reactive Black 5 solution with time, *t*. An amount of 5 mg of Reactive Black 5 and 50 mg of polypyrrole nanofibers in 50 mL of water at 20 °C [16].

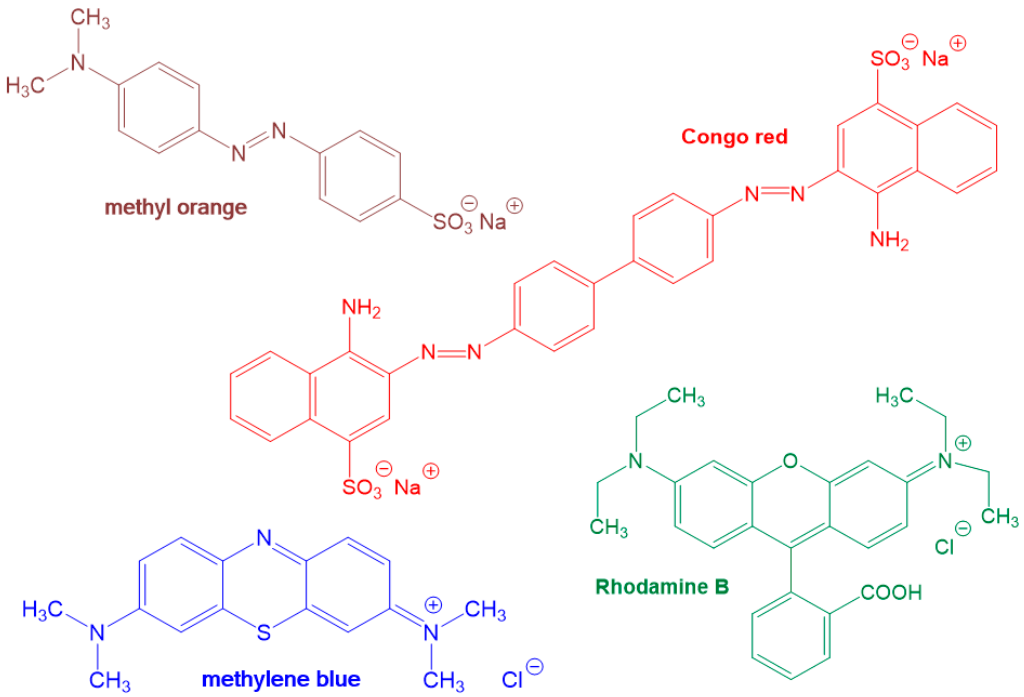

Figure 8. The most often used anionic (**top**: methyl orange, Congo red) and cationic dyes (**bottom**: methylene blue and Rhodamine B).

The experimental data and the time dependence of the dye concentration decrease are often interpreted in terms of various adsorption models: a pseudo-first-order, a pseudo-second-order, Freundlich, Langmuir, Temkin, or others. The authors found that one of them provided the best fit of the data, with the Langmuir isotherm being the most often winner [7,8,20–24]. This is the correct approach, but only if the dye removal mechanism is based exclusively on adsorption.

Only the removal of soluble organic dyes is reviewed below; however, the many adsorbents and experimental techniques can also be used for the removal of colored toxic heavy

metal compounds [3], such as lead(II) and cadmium(II) salts [25], chromium(VI) [26–29], and zinc(II) ions [30]. This also applies to the removal of various drugs, which may often be structurally related to the dyes, e.g., oxytetracycline [31], chloramphenicol or furazolidone [32], rifampin [33] as well as organic dyes. Such studies illustrate a more general application of the composites based on conducting polymers in waste water remediation.

2. Polyaniline Adsorbents

Polyaniline alone has been recently tested as an adsorbent in several papers. It was applied to the adsorption of cationic dye, Basic Red 46 [20]. Polyaniline, prepared with two different oxidants, ammonium peroxydisulfate, and manganese dioxide, hesitantly adsorbed methylene blue to the same extent and more efficiently than Reactive Black 5 [34]. Polyaniline, prepared with iron(III) chloride oxidant, was used to adsorb Acid Red G [35]. Another type of polyaniline, prepared in the absence of acid and containing aniline oligomers, adsorbed methylene blue and indigo carmine [36]. Polyaniline, prepared in the presence of amino acids, was tested for the adsorption of Congo red [37]. The same dye and Rhodamine B were adsorbed with hollow polyaniline microspheres [38]. A polyaniline base was used for the adsorption of methylene blue [39]. The reports on the adsorption of neat polyaniline as a reference material can also be found in various papers dealing with polyaniline composites, e.g., [9,22,40,41].

2.1. Binary Polyaniline Composites

Conducting polymers are useful for the fundamental investigation of interactions with conducting polymers. For practical applications, however, conducting composites are required. This means that additional material is introduced to the conducting polymers that afford mechanical or other material properties suitable for the particular application, such as gel-like or macroporous substances [16,42,43]. They affect the distribution of conducting polymer within the composite and the access of organic dyes to adsorption sites. The independent adsorption of dyes on the supporting substrate must also be considered. The non-conducting component may act as an independent adsorbent, e.g., melamine sponge [16], that may improve or broaden dye removal ability.

The simple binary composites are usually prepared by an in situ deposition of conducting polymers on the substrates immersed in a reaction mixture used for conducting polymer preparations, i.e., they are of a core–shell type (Table 1). This is based on the observation that any material in contact with the reaction mixture becomes coated with a thin submicrometre film [44], which is well suited for adsorption purposes. The coating of inorganic substrates is represented by the following: barium titanate [45]; cobalt ferrite [28]; cobalt sulfide [46]; copper(II) oxide [47]; fly ash [48]; iron oxyhydroxide [49]; iron sulfide [21]; magnetite [50]; manganese(IV) dioxide [34,40]; manganese ferrite [51]; magnesium ferrite [52]; molybdenum trioxide [53]; montmorillonite [54]; nickel oxide [40]; silica gel [55]; tin dioxide [56]; titanium dioxide [22,33,57,58]; zeolite [59]; zinc oxide [60–62]; zirconium(IV) dioxide [63].

Table 1. Polyaniline composites applied as dye adsorbents [a].

Dye		PANI Composite with	Reference
BINARY COMPOSITES			
Acid Blue 74	–	Tea saponin	[41]
Acid Red 18	–	$CoFe_2O_4$	[28]
Brilliant green	+	Reduced graphene oxide	[69]
Brilliant green	+	SiO_2	[55]
Congo red	–	Activated carbon	[66]

Table 1. *Cont.*

Dye		PANI Composite with	Reference
		$BaTiO_3$	[72]
		Graphene	[68]
		Kevlar fibers	[73]
		Polyimide	[74]
		SiO_2	[55]
		Tea saponin	[41]
		TiO_2	[58]
		ZnO	[60]
Crystal violet	+	SiO_2	[55]
Direct Blue 14	−	Activated carbon	[64]
		Polystyrene	[64]
Direct Blue 15	−	SnO_2	[56]
Eosin Y	−	FeS	[21]
Methyl orange	−	Activated carbon	[7]
		Bacterial cellulose	[75]
		Cellulose	[24]
		CuO	[71]
		Fe_3O_4	[50]
		Manganese ferrite	[51]
		Multiwall carbon nanotubes	[8]
		PEO	[76]
		Polyurethane foam	[77]
		TiO_2	[22]
Methyl red	−	$MgFe_2O_4$	[52]
Methylene blue	+	Boron cluster	[27]
		Carbonized peanut shells	[65]
		CMC	[78]
		MnO_2	[34]
		Poly(phenyl sulfone)	[79]
		Reduced graphene oxide	[30]
		ZnO	[60]
		ZnO/SiO_2	[62]
		ZrO_2	[63]
		Cellulose	[24]
Mordant Blue 9	−	CMC	[78]
Orange G	−	Opuntia ficus	[80]
		Nut shells	[81]
		Zeolite	[59]
Orange II	−	FeO(OH)	[49]
Reactive Black 5	−	Manganese dioxide	[34]

Table 1. *Cont.*

Dye		PANI Composite with	Reference
Reactive Green 19	−	Montmorillonite	[54]
4Rhodamine 6G	+	Boron cluster	[27]
Rhodamine B	+	Carbonized tea waste	[67]
		CMC	[78]
Sunset yellow	−	Reduced graphene oxide	[30]
		TERNARY COMPOSITES	
Allura Red	−	Bentonite/PEO	[40]
Congo red	−	CoS/graphite	[46]
		Fly ash/Fe_3O_4	[48]
		L-cysteine/reduced graphene oxide	[70]
Crystal violet	+	Fe_3O_4/chitosan	[82]
Methyl orange	−	Cu/TiO_2	[22]
		Fe_3O_4/chitosan	[82]
		Fly ash/Fe_3O_4	[48]
		MnO_2/NiO	[40]
		Montmorillonite/PVAL	[43]
		PAA/PAN	[83]
		SiO_2	[55]
		TiO_2/PVDF	[84]
		TiO_2/PVDF	[85]
Methylene blue	+	MoO_3/Fe_3O_4	[53]
		PAA/PAN	[83]
Orange G	−	Calcium alginate/sawdust	[86]
Reactive Black 5	−	Montmorillonite/PVAL	[43]
		Fe_3O_4/PVAL	[42]
Reactive Orange 5	−	TiO_2/zeolite	[33]
Rhodamine B	+	CuO/graphene	[47]
Safranin	+	Montmorillonite/PVAL	[43]

[a] The plus sign + denotes a cationic dye, and the minus sign − is an anionic one. The same notation is used in all Tables. CMC = carboxymethylcellulose; PAA = poly(acrylic acid); PAN = polyacrylonitrile; PEO = poly(ethylene oxide); PVAL = poly(vinyl alcohol); PVDF = poly(vinylidene fluoride).

A separate class of adsorbents is represented by the polyaniline-coated carbonaceous materials, e.g., activated carbon [7,64]; activated carbonized peanut shells [65]; activated carbons based on prickly pear seeds [66]; carbonized tea waste [67]; graphene [47,68]; multiwall carbon nanotubes [8] or reduced graphene oxide [30,69,70]. Only exceptionally, polyaniline was decorated in a reverse manner by an inorganic component, such as copper(II) oxide [71].

It should be mentioned that some inorganic compounds, typically titanium dioxide or zinc oxide but also others, are also active as photocatalysts. This means that the dye removal reported as adsorption may contain a contribution of photocatalytic decomposition. This also applies vice versa: prior adsorption of the dye on a photocatalyst is needed for

photocatalytic degradation. For the practical application, it need not be important which mechanism of dye removal, adsorption, or photodegradation predominates.

The organic substrates coated with conducting polymers include synthetic polymers, such as carboxymethylcellulose gel [78], Kevlar fibers [73], macroporous melamine sponges [16], poly(ethylene oxide) [76], polyimide membrane [74], polystyrene [64], poly(vinyl alcohol) aerogel [42], polyurethane foam [77], and various natural materials, such as [24,75], chitosan [82], opuntia ficus [80], almond and wall nut shells [81] or tea saponin [41]. Only exceptionally, both components were simply mixed, e.g., polyaniline and nitrogen-containing carbon nanodots [87] or zinc oxide [61]. In this case, the fact that the organic component may also be an efficient adsorbent in addition to conducting polymer also has to be kept in mind [16].

The removal of dyes by the hybrid inorganic–organic composites was more efficient when compared with neat polyaniline and inorganic component alone [7,8,41,72,88]. This is interpreted as a synergistic effect, but a few words of explanation are relevant. Polyaniline is prepared in globular form (Figure 9) with closely packed chains cross-linked by hydrogen bonding to nitrogen atoms. When polyaniline is deposited on a particulate substrate in situ during the polymer preparation, thin submicrometre polyaniline film grows on the substrate's surface. It is assumed that the polyaniline chains are more organized and grow in a perpendicular direction to the coated surface. The resulting brush-like morphology may be better penetrable to the dye molecules, and also, the specific surface area of polyaniline in coatings will be larger than that in the compact globules. For this reason, the hybrid coatings perform better as adsorbents than individual components. The observed "synergism" is not a result of a specific interaction between the polyaniline and supporting materials, but it is due to the different morphology and random chain arrangement in the globular polyaniline and more ordered structure in the polyaniline coatings.

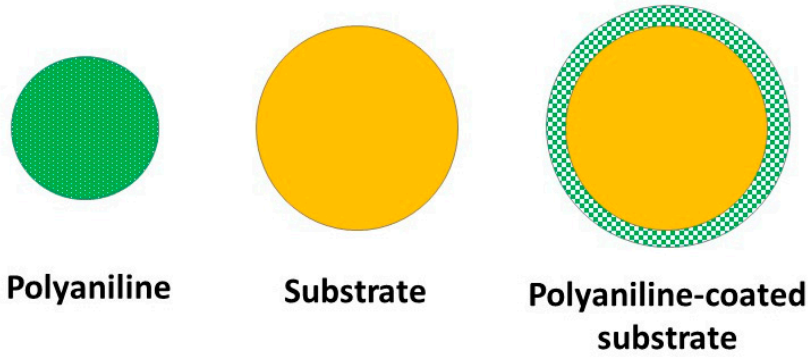

Figure 9. Globular polyaniline and polyaniline-coated substrate.

2.2. Ternary Polyaniline Composites

Multicomponent composites are composed of more than two components. Here, three is a typical number (Table 1). For example, they include some specific parts, such as magnetite or ferrites [26,42,46,48,50,51,53,82,89,90], which serve the adsorbent separation with a magnetic field.

Poly(vinyl alcohol) supports the composite macroporosity when used in aerogels [42,43]. Calcium alginate hydrogel provided a matrix for polyaniline/sawdust [86]. A supporting polymer was also introduced when the adsorbent was a part of a membrane [40,74,76,79,83–85].

Many studies agree that polyaniline is an efficient adsorbent or photocatalyst for both anionic and cationic dyes [24,55,91,92], meaning that ionic interactions are not decisive in their activity.

3. Polyaniline Photocatalysts

There is a single report on the photocatalytic degradation of malachite green and methylene blue caused by polyaniline [93]. Polyaniline, however, was prepared by the oxidation of aniline with periodic acid in acetonitrile and not by the standard way using ammonium peroxydisulfate in an aqueous medium [5].

3.1. Binary Polyaniline Composites

The composites used for the photocatalytic decomposition of dyes have also displayed adsorption properties [94] because dye adsorption on a photocatalyst is the prerequisite for efficient photocatalytic dye decomposition. The composites typically contained an inorganic photocatalyst, a conducting polymer, and a supporting material (Table 2). The inorganic component was coated with conducting polymer in situ during the synthesis of polyaniline (Figure 9). A polyaniline coating has a typical thickness of 100–200 nm and is green; however, it is still sufficiently transparent to all wavelengths of the UV-visible light, which thus has access to the photocatalyst. This is important for the success of photocatalysis afforded by hybrid composites.

Table 2. Polyaniline composites applied as photocatalysts.

Dye		PANI Composite with	Reference
BINARY COMPOSITES			
Acid Blue 29	–	CdS	[97]
Acid Orange 52	–	TiO_2	[105]
Brilliant green	+	Ni	[100]
Congo red	–	Carbon nanodots	[87]
		g-C_3N_4	[98]
		Reduced graphene oxide	[101]
		ZrO_2	[9]
Crystal violet	+	Carbon nanodots	[87]
		$NiWO_4$	[111]
Disperse Red 1	–	$Co_{0.5}Zn_{0.5}Fe_2O_4$	[90]
Fluorescein	–	ZnO	[108]
Levafix red	–	Fe_3O_4	[89]
Malachite green	+	Fe_3O_4	[89]
Methyl orange	–	Ag_2O	[102]
		g-C_3N_4	[98]
		MWCNT	[99]
		TiO_2	[106]
Methylene blue	+	Carbon nanodots	[87]
		MWCNT	[99]
		Nb_2O_5	[101]
		$NiWO_4$	[111]
		TiO_2	[104]
		ZnO	[61]
Orange II	–	ZnO	[109]
Reactive Blue 220	–	BiOCl	[95]
Reactive Orange 14	–	$Co_{0.5}Zn_{0.5}Fe_2O_4$	[90]
Rhodamine B	+	Carbon nanodots	[87]
		CdS	[96]
		MWCNT	[99]

Table 2. *Cont.*

Dye		PANI Composite with	Reference
		SnO_2	[103]
		WO_3	[107]
		TERNARY COMPOSITES	
Acid Blue 29	–	TiO_2/CdS	[97]
Allura red	–	TiO_2/PVDF	[84]
Congo red	–	Zn/Fe_3O_4	[118]
Methyl orange	–	Ag/$AgMoO_4$	[29]
		g-C_3N_4/attapulgite	[112]
		TiO_2/chitosan	[115]
		TiO_2/PVDF	[84]
Methyl red	–	ZnO/Cu/Ni	[110]
Methylene blue	+	CeO_2/polystyrene	[113]
		TiO_2/chitosan	[115]
		ZnO/graphene oxide	[116]
Methylene green	+	$NaBiO_2$/polycarbonate	[114]
Reactive Black 5	–	TiO_2/Fe_3O_4	[117]
Reactive Brilliant Red K-2K	–	Graphene oxide/cellulose	[94]
Rhodamine B	+	BiOI/reduced graphene oxide	[10]
		$NaBiO_2$/polycarbonate	[114]

The list of simple polyaniline composites includes the following moieties: bismuth oxychloride [95]; cadmium sulfide [96,97]; carbon nitride [98]; magnetite [89]; multiwall carbon nanotubes [99]; nickel [100]; reduced graphene oxide [101]; silver molybdate [29]; silver oxide [102]; tin dioxide [103]; titanium dioxide [104–106]; tungsten trioxide [107]; zinc oxide [61,104,108–110]; zirconium dioxide [9].

In the preparation of the above composites, the inorganic substrate was coated with polyaniline in the course of its preparation. On rare occasions, polyaniline was simply mixed with an inorganic compound. The mixture of polyaniline and nitrogen-containing carbon nanodots, obtained by the hydrothermal method from bovine serum albumin, photocatalyzed the decomposition of various dyes [87]. A mixture of commercial polyaniline with nickel tungstate was used to decompose methylene blue and crystal violet [111].

3.2. Ternary Polyaniline Composites

Ternary systems are more useful for practical applications (Table 2) but also more difficult to interpret because each component can participate in dye adsorption. The latest examples are: attapulgite/*g*-carbon nitride [112]; bismuth(III) oxyiodide/reduced graphene oxide [10]; cerium dioxide/polystyrene [113]; cobalt/zinc ferrite [90]; sodium bismuthate/polycarbonate [114]; titanium dioxide/cadmium sulfide [97]; titanium dioxide/chitosan [115]; titanium dioxide/poly(vinylidene fluoride) [84,85]; zinc oxide/graphene oxide/viscose [116]; zinc/magnetite [117,118].

The antibacterial activity of the polyaniline composites has occasionally been mentioned [56,75,78,101]. This may be expected, especially in photocatalytic experiments, due to the formation of reactive oxygen species [87,119,120].

4. Polypyrrole Adsorbents

The adsorption or an anionic dye, Reactive Black 5, on globular polypyrrole was poor, but it was complete when the polypyrrole nanofibers of nanotubes were used instead [16]. In another study, the adsorption of both anionic and cationic dyes was attributed to electrostatic interactions and hydrogen bonding [12].

4.1. Binary Polypyrrole Composites

In contrast to polyaniline, polypyrrole composites have been investigated as adsorbents less often (Table 3). Polypyrrole has been combined and, as a rule, deposited in situ during the polymerization of pyrrole onto inorganic substrates, such as carbon nitride [121], MXene [122], nanosilica [23], and stainless steel mesh [123].

Table 3. Polypyrrole composites applied as dye adsorbents [a].

Dye		Composite with	Reference
		BINARY COMPOSITES	
Acid Orange 7	–	nanosilica	[23]
alizarine red	–	carbonized chicken feathers	[126]
chrysoidine	+	melamine	[16]
Congo red	–	Chinese yam peel	[127]
		PPT	[124]
Eosin Y	–	PPT	[124]
		wheat straw	[128]
fuchsin	–	bacterial cellulose	[125]
malachite green	+	steel mesh	[123]
methyl orange	–	MXene	[122]
methylene blue	+	*g*-C_3N4	[121]
		MXene	[122]
		sodium alginate	[129]
Reactive Black 5	–	melamine	[15–18]
Rhodamine B	+	*g*-C_3N4	[121]
		steel mesh	[123]
		TERNARY COMPOSITES	
Acid Orange 7	–	PAN/PVP nanofibers	[131]
Acid Yellow 9	–	PAN/PVP nanofibers	[131]
Congo red	–	CoO/graphene	[25]
		PEGMA/Fe_3O_4	[132]
		sodium alginate/algae biomass	[130]
metanil yellow	–	PAN/PVP nanofibers	[131]
methyl orange	–	magnetite/chitosan	[26]
methylene blue	+	CoO/graphene	[25]
		MoO_3/Fe_3O_4	[53]

[a] PAN = polyacrylonitrile; PVP = poly(*N*-vinylpyrrolidone); PEGMA = poly(ethyleneglycol methacrylate); PPT = poly(*p*-phenylene terephthamide).

Organic supports, such as melamine sponge [16] and poly(*p*-phenylene terephthalamide) [124], have been used to provide macroporous sponges or membranes. Additionally,

natural organics have been used to provide a value-added material, e.g., bacterial cellulose [125], carbonized chicken feathers [126], Chinese yam peel [127], and wheat straw [128].

In the systems comprising polypyrrole, the morphology of this polymer, as globules or nanotubes (Figure 5), has to be taken into account. Globular polypyrrole, deposited on macroporous melamine sponge, did not significantly adsorb Reactive Black 5 [16], but polypyrrole nanotubes on the same substrate proved to be an excellent adsorbent of this dye [15,16]. This may be the result of a better polymer chain organization in nanotubes compared to the random arrangement in globules, similar to polyaniline (Figure 9). The polypyrrole nanotubes had a higher conductivity, specific surface area, and stability with respect to the acidity changes when compared with the globular form [11,13]. The adsorption decreased after coating with polypyrrole. Melamine sponge alone was not indifferent; however, it efficiently adsorbed a cationic dye, crystal violet, meaning that the adsorption properties of the support also have to be considered.

In general, only limited attention has been paid to the composites of polypyrrole nanotubes. Wheat straw biomass was coated in situ with the polypyrrole nanotubes and used for the removal of Eosin Y [128]. The polypyrrole nanotubes were dispersed in sodium alginate gel and then applied for the removal of methylene blue [129].

4.2. Ternary Polypyrrole Composites

The typical adsorbents had three components again: a conducting polymer, an inorganic compound, and a supporting material (Table 3). Cobalt oxide/graphene [25] and molybdenum trioxide/magnetite [53] are examples of inorganic components, while the organics are represented by sodium alginate/algae biomass [130], polyacrylonitrile/poly(*N*-vinylpyrrolidone) [131], and poly(ethyleneglycol methacrylate)/magnetite microspheres [132].

5. Polypyrrole Photocatalysts

The photocatalytic activity of polypyrrole alone was reported only rarely and was demonstrated in the removal of methyl orange [133] and malachite green [134]. The main reactive species generated under illumination were identified to be oxygen anion-radicals.

5.1. Binary Polypyrrole Composites

In addition to polypyrrole, the simple binary composites contained inorganic components (Table 4). The improvement in the catalytic activity has often been observed after the surface modification with a conducting polymer.

Table 4. Polypyrrole composites applied as dye photocatalysts.

Dye		Composite with	Reference
BINARY COMPOSITES			
alizarine red	–	$FeWO_4$	[135]
Congo red	–	$MoSe_2$	[92]
malachite green	+	Fe	[134]
methyl orange	–	$AgMnO_2$	[32]
		TiO_2	[58]
methylene blue	+	Ag	[137]
	+	MWCNT	[136]
	+	WO_3	[138]
Rhodamine B	+	$MoSe_2$	[92]
	+	MWCNT	[136]

Table 4. *Cont.*

Dye		Composite with	Reference
rose bengal	–	$FeWO_4$	[135]
		TERNARY COMPOSITES	
brilliant red	–	*g*-C_3N_4/reduced graphene oxide	[119]
Congo red	–	Ag/Sn_3O_4	[120]
malachite green	+	Ag/ZnO	[142]
	+	Ag/ZnO/cellulose acetate	[141]
metanil yellow	–	CuO/ZnO	[143]
methyl orange	–	MWCNT/polyacrylonitrile	[139]
		TiO_2/Cu-MOF	[91]
methylene blue	+	TiO_2/graphene oxide	[140]
		Ag/Sn_3O_4	[120]
		TiO_2/Cu-MOF	[91]
		ZnO/activated carbon	[141]
		ZnO/Fe_3O_4	[19]
Rhodamine B	+	MWCNT/polyacrylonitrile	[139]
		TiO_2/Cu-MOF	[91]

The substrates used for the deposition of polypyrrole were as follows: iron [134]; iron tungstate [135]; molybdenum sulfide [92]; MWCNT [136]; silver [137]; silver manganite [32]; titanium dioxide [58]; or tungsten trioxide [138].

5.2. Ternary Polypyrrole Composites

Most studies, however, have been devoted to multicomponent composite materials (Table 4). The ternary composites typically included photocatalytically active inorganic compounds, e.g., titanium dioxide or zinc oxide. A third component has often been included, typically a polymer, to provide materials with a controlled morphology or mechanical properties required by applications.

A list of the composites used in the recent literature includes: graphitic carbon/reduced graphene oxide composites [119]; multiwall carbon nanotubes/polyacrylonitrile [139]; silver/tin oxide [120]; titanium dioxide/Cu-MOF [91]; titanium dioxide/graphene oxide [140]; zinc oxide/activated carbon [72]; zinc oxide/cellulose acetate [141,142]; zinc oxide/copper [143]; or zinc oxide/magnetite [19].

6. Polyaniline and Polypyrrole Derivatives

Substituted polyanilines have been used in dye removal, but only exceptionally. The poly(*N*-methylaniline)/chitosan composite was used for methyl red removal [144]. Polyphenylenediamines [145] are promising candidates for adsorbents due to their preparation from non-toxic monomers at an economical cost. They are considerably less conducting compared with polyaniline, but this need not be a drawback in dye removal. Poly-*p*-phenylenediamine, deposited on hydrolyzed polyacrylonitrile membrane, has recently been reported to remove the anionic Congo red and Direct Red 23 dyes [146].

Polyaniline can easily be converted to nitrogen-containing carbons [147]. The morphology is retained after this process, except for some shrinkage. Carbon fibers prepared from the polyaniline precursor were combined with titanium dioxide to produce a photocatalyst for the decomposition of methylene blue [148].

The study that combined both of our reviewed conducting polymers, polyaniline, and polypyrrole, in the composite with carbon nitride involved methylene blue as the decomposition object [149].

Concerning polypyrrole, there are many ways to modify the polymer chains by copolymerization with ring-substituted monomers; however, reports in this direction are scarce. For example, poly(pyrrole-*co*-sulfophenylenediamine) was found to adsorb an anionic dye, Congo red, and a cationic dye, methylene blue [150].

Polypyrrole was exposed to 200, 400, and 650 °C in an inert atmosphere. This first deprotonated polypyrrole (Figure 4), followed by its carbonization [151,152]. The ability to remove Reactive Black 5 from aqueous media decreased with an increasing exposure temperature. The activation of polypyrrole with potassium hydroxide during pyrolysis only slightly increased the adsorption ability [152].

7. Conclusions

The conducting polymers, polyaniline, and polypyrrole, became well-established active materials for wastewater management. In recent years, from 2020 to 2022, most papers have been dedicated to the application of polyaniline as a dye adsorbent (Table 1). A preference was given to the anionic dyes, where the electrostatic interaction with polymer cations was expected. In the photocatalytic studies, the participation of the anionic and cationic dyes was balanced (Table 2). The number of papers reporting on polypyrrole was slightly lower with regards to the comparable treatment of anionic and cationic dyes both in adsorption (Table 3) and photocatalytic decomposition (Table 4). Still, more detailed studies on neat polyaniline and polypyrrole, even though of academic interest, would be welcome to further our understanding of the role of these polymers in the composites for practical application. Concerning the mechanism of dye removal, dye adsorption, or photocatalytic decomposition, they are likely to be operative at the same time, and their contributions should be estimated if possible. It has to be stressed that the present review concerns the papers published in 2020–2022. For the extensive work reported in preceding years, the readers are referred to an earlier review [1].

8. Future Prospects

Conducting polymers are not just conducting [153]. Their use as adsorbents of organic dyes is a typical example of an application that does not require electrical conductivity. However, in the next step, their conductivity allows for the construction of electrodes by their in situ deposition on non-conducting substrates and subsequent use in electrochemistry. In this experiment, an electric potential was applied to the conducting polymer adsorbent. The electrochemical switching between the redox polymer forms may change the adsorption properties due to a change in molecular structure, degree of protonation, and/or hydrophilicity. For example, the electroremediation of aqueous effluents containing Congo red on polyaniline/titanium dioxide composite points in this direction [58], similar to the electrooxidation of this dye on the polyimide membrane coated with polyaniline [74]. Such systems might be regarded as intelligent adsorbents controlled by the applied potential.

The array of adsorbents may be broadened by testing the polymers of ring-substituted anilines, viz., phenylenediamines [145] and various copolymers, with aniline. As a rule, they have a lower conductivity than polyaniline, but this would not limit their suitability for dye removal experiments. Concerning polypyrrole, attention should be paid to its morphology, especially to the nanotubes, which have been tested only marginally.

Funding: The support of the Ministry of Education, Youth and Sports of the Czech Republic (FSR AD 70202001026/1100) is gratefully acknowledged.

Conflicts of Interest: The author declares no conflict of interest.

References

1. Stejskal, J. Interaction of conducting polymers, polyaniline and polypyrrole, with organic dyes: Polymer morphology control, dye adsorption and photocatalytic decomposition. *Chem. Pap.* **2020**, *74*, 1–54. [CrossRef]
2. Ambigadevi, J.; Kumar, P.S.; Vo, D.-V.N.; Haran, S.H.; Raghavan, T.S. Recent developments in photocatalytic remediation of textile effluent using semiconductor based nanostructured catalyst: A review. *J. Environ. Chem. Eng.* **2020**, *9*, 104881. [CrossRef]
3. Senguttuvan, S.; Senthilkumar, P.; Janaki, V.; Kamala-Kannan, S. Significance of conducting polyaniline based composites for the removal of dyes and heavy metals from aqueous solution and wastewaters—A review. *Chemosphere* **2020**, *267*, 129201. [CrossRef]
4. Khan, M.; Ali, S.W.; Shahadat, M.; Sagadevan, S. Applications of polyaniline-impregnated silica gel-based nanocomposites in wastewater treatment as an efficient adsorbent of some important organic dyes. *Green Process. Synth.* **2022**, *11*, 617–630. [CrossRef]
5. Sapurina, I.; Stejskal, J. The mechanism of the oxidative polymerization of aniline and the formation of supramolecular polyaniline structures. *Polym. Int.* **2008**, *57*, 1295–1325. [CrossRef]
6. Stejskal, J.; Gilbert, R.G. Polyaniline. Preparation of a conducting polymer (IUPAC Technical Report). *Pure Appl. Chem.* **2002**, *74*, 857–867. [CrossRef]
7. Bekhoukh, A.; Moulefera, I.; Zeggai, F.Z.; Benyoucef, A.; Bachari, K. Anionic methyl orange removal from aqueous solutions by activated carbon reinforced conducting polyaniline as adsorbent: Synthesis, characterization, adsorption behavior, regeneration and kinetics study. *J. Polym. Environ.* **2021**, *30*, 886–895. [CrossRef]
8. Maeda, S.; Armes, S.P. Surface-area measurements on conducting polymer-inorganic oxide nanocomposites. *Synth. Met.* **1995**, *73*, 151–155. [CrossRef]
9. Zor, S.; Budak, B. Photocatalytic degradation of congo red by using PANI and PANI/ZrO_2: Under UV-A light irradiation and dark environmental. *Desalination Water Treat.* **2020**, *201*, 420–430. [CrossRef]
10. Wang, X.; Zhu, J.; Yu, X.; Fu, X.; Zhu, Y.; Zhang, Y. Enhanced removal of organic pollutant by separable and recyclable rGH-PANI/BiOI photocatalyst via the synergism of adsorption and photocatalytic degradation under visible light. *J. Mater. Sci. Technol.* **2020**, *77*, 19–27. [CrossRef]
11. Stejskal, J.; Trchová, M.; Bober, P.; Morávková, Z.; Kopecký, D.; Vrňata, M.; Prokeš, J.; Varga, M.; Watzlová, E. Polypyrrole salts and bases: Superior conductivity of nanotubes and their stability towards the loss of conductivity by deprotonation. *RSC Adv.* **2016**, *6*, 88382–88391. [CrossRef]
12. Ji, Y.; Zhang, W.; Yang, H.; Ma, F.; Xu, F. Green synthesis of poly(pyrrole methane) for enhanced adsorption of anionic and cationic dyes from aqueous solution. *J. Colloid Interface Sci.* **2021**, *590*, 396–406. [CrossRef] [PubMed]
13. Stejskal, J.; Trchová, M. Conducting polypyrrole nanotubes: A review. *Chem. Pap.* **2018**, *72*, 1563–1595. [CrossRef]
14. Stejskal, J.; Prokeš, J. Conductivity and morphology of polyaniline and polypyrrole prepared in the presence of organic dyes. *Synth. Met.* **2020**, *264*, 116373. [CrossRef]
15. Stejskal, J.; Sapurina, I.; Vilčáková, J.; Humpolíček, P.; Truong, T.H.; Shishov, M.A.; Trchová, M.; Kopecký, D.; Kolská, Z.; Prokeš, J.; et al. Conducting polypyrrole-coated macroporous melamine sponges: A simple toy or an advanced material? *Chem. Pap.* **2021**, *75*, 5035–5055. [CrossRef]
16. Stejskal, J.; Pekárek, M.; Trchová, M.; Kolská, Z. Adsorption of organic dyes on macroporous melamine sponge incorporating conducting polypyrrole nanotubes. *J. Appl. Polym. Sci.* **2022**, *139*, 52156. [CrossRef]
17. Pete, S.; Kattil, R.A.; Thomas, L. Polyaniline-multiwalled carbon nanotubes (PANI-MWCNTs) composite revisited: An efficient and reusable material for methyl orange dye removal. *Diam. Relat. Mater.* **2021**, *117*, 108455. [CrossRef]
18. Stejskal, J.; Kopecký, D.; Kasparyan, H.; Vilčáková, J.; Prokeš, J.; Křivka, I. Melamine sponges decorated with polypyrrole nanotubes as macroporous conducting pressure sensors. *ACS Appl. Nano Mater.* **2021**, *4*, 7513–7519. [CrossRef]
19. Nayebi, P.; Babamoradi, M. Synthesis of ZnO nanorods/Fe_3O_4/Polypyrrole nanocomposites for photocatalytic activity under the visible light irradiation. *Optik* **2021**, *244*, 167497. [CrossRef]
20. Jadhav, S.; Jaspal, D. Elimination of cationic azodye from aqueous media using doped polyaniline (PANI): Adsorption optimization and modeling. *Can. J. Chem.* **2020**, *98*, 717–724. [CrossRef]
21. Danu, B.Y.; Agorku, E.S.; Ampong, F.K.; Awudza, J.A.M.; Torve, V.; Danquah, I.M.K.; Ama, O.M.; Osifo, P.O.; Ray, S.S. Iron sulfide functionalized polyaniline nanocomposite for the removal of Eosin Y from water: Equilibrium and kinetic studies. *Polym. Sci. Ser. B* **2021**, *63*, 304–313. [CrossRef]
22. Khairy, M.; Kamar, E.M.; Yehia, M.; Masoud, K.M. High removal efficiency of methyl orange dye by pure and (Cu, N) doped TiO_2/polyaniline nanocomposites. *Biointerface Res. Appl. Chem.* **2021**, *12*, 893–909. [CrossRef]
23. Sillanpää, M.; Mahvi, A.H.; Balarak, D.; Khatibi, A.D. Adsorption of Acid Orange 7 dyes from aqueous solution using Polypyrrole/nanosilica composite: Experimental and modelling. *Int. J. Environ. Anal. Chem.* **2021**, 1–18. [CrossRef]
24. Nguyen, T.H.; Nguyen, M.T.; Vuong, B.H.; Le, T.H. Cellulose grafted with polyaniline for simultaneous adsorption of cationic and anionic dyes in wastewater effluent. *Cellulose* **2022**, *29*, 7761–7773. [CrossRef]
25. Anuma, S.; Mishra, P.; Bhat, B.R. Polypyrrole functionalized cobalt oxide graphene (COPYGO) nanocomposite for the efficient removal of dyes and heavy metal pollutants from aqueous effluents. *J. Hazard. Mater.* **2021**, *416*, 125929. [CrossRef]
26. Alsaiari, N.; Amari, A.; Katubi, K.; Alzahrani, F.; Rebah, F.; Tahoon, M. Innovative magnetite based polymeric nanocomposite for simultaneous removal of methyl orange and hexavalent chromium from water. *Processes* **2021**, *9*, 576. [CrossRef]
27. Li, X.; Zhao, X.; Li, X.; Jia, X.; Chang, F.; Zhang, H.; Hu, G. Rapid simultaneous removal of cationic dyes and Cr(VI) by boron cluster polyaniline with a target site. *Chem. Commun.* **2021**, *57*, 7569–7572. [CrossRef]

28. Mohammadi, H.; Ghaedi, M.; Fazeli, M.; Sabzehmeidani, M.M. Removal of hexavalent chromium ions and Acid Red 18 by superparamagnetic $CoFe_2O_4$/polyaniline nanocomposites under external ultrasonic fields. *Microporous Mesoporous Mater.* **2021**, *324*, 111275. [CrossRef]
29. Peng, D.-Y.; Zeng, H.-Y.; Xiong, J.; Xu, S.; An, D.S. Improved photocatalytic performance of p-n heterostructure Ag-Ag_2MoO_4/polyaniline for chromium (VI) reduction and dye degradation. *J. Alloy. Compd.* **2022**, *912*, 165063. [CrossRef]
30. Kuznetsova, T.S.; Burakova, I.V.; Pasko, T.V.; Burakov, A.E.; Melezhik, A.V.; Mkrtchyan, E.S.; Babkin, A.V.; Neskoromnaya, E.A.; Tkachev, A.G. Technology of nanocomposites preparation for sorption purification of aqueous media. *Inorg. Mater. Appl. Res.* **2022**, *13*, 434–441. [CrossRef]
31. Yu, C.; Tan, L.; Shen, S.; Fang, M.; Yang, L.; Fu, X.; Dong, S.; Sun, J. In situ preparation of *g*-C_3N_4/polyaniline hybrid composites with enhanced visible-light photocatalytic performance. *J. Environ. Sci.* **2021**, *104*, 317–325. [CrossRef]
32. Abinaya, M.; Muthuraj, V. Bi-functional catalytic performance of silver manganite/polypyrrole nanocomposite for electrocatalytic sensing and photocatalytic degradation. *Colloids Surf. A Physicochem. Eng. Asp.* **2020**, *604*, 125321. [CrossRef]
33. Motamedi, M.; Mollahosseini, A.; Negarestani, M. Ultrasonic-assisted batch operation for the adsorption of rifampin and reactive orange 5 onto engineered zeolite–polypyrrole/TiO_2 nanocomposite. *Int. J. Environ. Sci. Technol.* **2022**, *19*, 7547–7564. [CrossRef]
34. Sapurina, I.; Bubulinca, C.; Trchová, M.; Prokeš, J.; Stejskal, J. Solid manganese dioxide as heterogeneous oxidant of aniline in the preparation of conducting polyaniline or polyaniline/manganese dioxide composites. *Colloids Surf. A Physicochem. Eng. Asp.* **2022**, *638*, 128298. [CrossRef]
35. Lyu, W.; Yu, M.; Li, J.; Feng, J.; Yan, W. Adsorption of anionic acid red G dye on polyaniline nanofibers synthesized by $FeCl_3$ oxidant: Unravelling the role of synthetic conditions. *Colloids Surf. A Physicochem. Eng. Asp.* **2022**, *647*, 129203. [CrossRef]
36. Myasoedova, T.N.; Gadzhieva, V.A.; Miroshnichenko, Y.S. Properties of mesoporous pani nanorods obtained by facile acid-free synthesis as a sorbent for methylene blue and indigo carmine removal. *J. Polym. Res.* **2022**, *29*, 1–13. [CrossRef]
37. Zhao, Z.; Yang, Y.; Xu, L.; Qiu, Z.; Wang, Z.; Luo, Y.; Du, K. Amino acid-doped polyaniline nanotubes as efficient adsorbent for wastewater treatment. *J. Chem.* **2022**, *2022*, 2041512. [CrossRef]
38. Wu, Y.; Chang, H.; Peng, J.; Liu, Y.; Sun, B.; Yang, Z.; Gao, S.; Liu, F. A facile strategy to fabricate hollow spherical polyaniline and its application to dyes removal. *Polym. Bull.* **2022**, 1–14. [CrossRef]
39. Duhan, M.; Kaur, R. Nano-structured polyaniline as a potential adsorbent for methylene blue dye removal from effluent. *J. Compos. Sci.* **2021**, *5*, 7. [CrossRef]
40. Ali, L.I.A.; Ismail, H.K.; Alesary, H.F.; Aboul-Enein, H.Y. A nanocomposite based on polyaniline, nickel and manganese oxides for dye removal from aqueous solutions. *Int. J. Environ. Sci. Technol.* **2020**, *18*, 2031–2050. [CrossRef]
41. Zou, Z.J.; Li, Y.L.; Ma, Z.W.; Jin, Y.Q.; Lü, Q.F. Preparation and dye adsorption of low-cost polyaniline-tea saponin nanocomposites. *J. Wuhan Univ. Technol.-Mater. Sci. Ed.* **2021**, *36*, 546–556. [CrossRef]
42. Bober, P.; Minisy, I.; Acharya, U.; Pfleger, J.; Babayan, V.; Kazantseva, N.; Hodan, J.; Stejskal, J. Conducting polymer composite aerogel with magnetic properties for organic dye removal. *Synth. Met.* **2019**, *260*, 116266. [CrossRef]
43. Lyu, W.; Li, J.; Trchová, M.; Wang, G.; Liao, Y.; Bober, P.; Stejskal, J. Fabrication of polyaniline/poly(vinyl alcohol)/montmorillonite hybrid aerogels toward efficient adsorption of organic dye pollutants. *J. Hazard. Mater.* **2022**, *435*, 129004. [CrossRef] [PubMed]
44. Riede, A.; Helmstedt, M.; Sapurina, I.; Stejskal, J. In situ polymerized polyaniline films. Film formation in dispersion polymerization of aniline. *J. Colloid Interface Sci.* **2002**, *248*, 413–418. [CrossRef] [PubMed]
45. Singh, S.; Perween, S.; Ranjan, A. Dramatic enhancement in adsorption of Congo red dye in polymer-nanoparticle composite of polyaniline-zinc titanate. *J. Environ. Chem. Eng.* **2021**, *9*, 105149. [CrossRef]
46. Das, M.; Ray, P.G.; Dhara, S.; Roy, S. Symbiotically Augmented removal of Congo red by polyaniline/cobalt sulfide/graphite composites. *Mater. Chem. Phys.* **2021**, *278*, 125487. [CrossRef]
47. Zhang, T.; Huang, H.; Zhang, W.; Lu, Z.; Shen, M.; Liu, T.; Bai, J.; Yang, Y.; Zhang, J. Free-standing hybrid film for separation of dye pollutant with self-cleaning ability under visible light. *Chemosphere* **2021**, *291*, 132725. [CrossRef] [PubMed]
48. Li, D.W.; Tao, Y.L.; Li, S.; Wu, Y.N.; Wang, C.R.; Lv, Y.R.; Zhu, G.S.; Qiu, H.F.; Liu, X.; Chen, C. Porous cage-like microfiber of fly ash magnetic powder (CMS)/polyaniline (PANI) composites with absorption properties. *Phys. Scripta* **2022**, *97*, 085817. [CrossRef]
49. Xiong, H.; Zhang, B.; Cui, C.; Xu, Y. Polyaniline/FeOOH composite for removal of Acid Orange II from aqueous solutions. *Mater. Chem. Phys.* **2022**, *278*, 125701. [CrossRef]
50. Momina; Ahmad, K. Remediation of anionic dye from aqueous solution through adsorption on polyaniline/FO nanocomposite-modelling by artificial neural network (ANN). *J. Mol. Liq.* **2022**, *360*, 119497. [CrossRef]
51. Das, P.; Nisa, S.; Debnath, A.; Saha, B. Enhanced adsorptive removal of toxic anionic dye by novel magnetic polymeric nanocomposite: Optimization of process parameters. *J. Dispers. Sci. Technol.* **2020**, *43*, 880–895. [CrossRef]
52. Das, P.; Debnath, A. Fabrication of $MgFe_2O_4$/polyaniline nanocomposite for amputation of methyl red dye from water: Isotherm modeling, kinetic and cost analysis. *J. Dispers. Sci. Technol.* **2022**, 1–12. [CrossRef]
53. Fanourakis, S.K.; Barroga, S.Q.; Perez, J.V.D.; He, L.; Rodrigues, D.F. In situ polymerization of polypyrrole and polyaniline on the surface of magnetic molybdenum trioxide nanoparticles: Implications for water treatment. *ACS Appl. Nano Mater.* **2021**, *4*, 12415–12428. [CrossRef]
54. Peng, L.-G.; Zhao, P.; Cheng, H.-Q.; He, Q.-R.; Wang, X.-H.; Liu, J.-X.; Wang, J.-L. Adsorption Studies of Reactive Green 19 from Aqueous Solutions by Polyaniline/Montmorillonite Nanocomposite. *Sci. Adv. Mater.* **2022**, *14*, 535–544. [CrossRef]

55. Tanweer, M.S.; Iqbal, Z.; Alam, M. Experimental insights into mesoporous polyaniline-based nanocomposites for anionic and cationic dye removal. *Langmuir* **2022**, *38*, 8837–8853. [CrossRef]
56. Rajaji, U.; Rani, S.E.G.D.; Chen, S.M.; Rajakumar, K.; Govindasamy, M.; Alzahrani, F.M.; Alsaiari, N.S.; Ouladsmane, M.; Lydia, I.S. Synergistic photocatalytic activity of SnO_2/PANI nanocomposite for the removal of direct blue 15 under UV light irradiation. *Ceramics Int.* **2021**, *47*, 29225–29231. [CrossRef]
57. Lee, Y.-J.; Lee, H.S.; Lee, C.-G.; Park, S.-J.; Lee, J.; Jung, S.; Shin, G.-A. Application of PANI/TiO_2 composite for photocatalytic degradation of contaminants from aqueous solution. *Appl. Sci.* **2020**, *10*, 6710. [CrossRef]
58. Maldonado-Larios, L.; Mayen-Mondragón, R.; Martínez-Orozco, R.; Páramo-García, U.; Gallardo-Rivas, N.; García-Alamilla, R. Electrochemically-assisted fabrication of titanium-dioxide/polyaniline nanocomposite films for the electroremediation of congo red in aqueous effluents. *Synth. Met.* **2020**, *268*, 116464. [CrossRef]
59. Imgharn, A.; Anchoum, L.; Hsini, A.; Naciri, Y.; Laabd, M.; Mobarak, M.; Aarab, N.; Bouziani, A.; Szunerits, S.; Boukherroub, R.; et al. Effectiveness of a novel polyaniline@Fe-ZSM-5 hybrid composite for Orange G dye removal from aqueous media: Experimental study and advanced statistical physics insights. *Chemosphere* **2022**, *295*, 133786. [CrossRef]
60. Toumi, I.; Djelad, H.; Chouli, F.; Benyoucef, A. Synthesis of PANI@ZnO hybrid material and evaluations in adsorption of Congo red and methylene blue dyes: Structural characterization and adsorption performance. *J. Inorg. Organomet. Polym. Mater.* **2021**, *32*, 112–121. [CrossRef]
61. Turkten, N.; Karatas, Y.; Bekbolet, M. Preparation of PANI Modified ZnO Composites via different methods: Structural, morphological and photocatalytic properties. *Water* **2021**, *13*, 1025. [CrossRef]
62. Benchikh, I.; Dahou, F.Z.; Lahreche, S.; Sabantina, L.; Benmimoun, Y.; Benyoucef, A. Development and characterisation of novel hybrid materials of modified ZnO-SiO_2 and polyaniline for adsorption of organic dyes. *Int. J. Environ. Anal. Chem.* **2022**, 1–20. [CrossRef]
63. Kumar, N.; Bahl, T.; Kumar, R. Study of the methylene blue adsorption mechanism using ZrO_2/Polyaniline nanocomposite. *Nano Express* **2020**, *1*, 030025. [CrossRef]
64. Eisazadeh, N.; Eisazadeh, H.; Ghadakpour, M. Comparison between various adsorbents for Direct Blue dye 14 removal from aqueous solution. *Fibers Polym.* **2021**, *22*, 149–158. [CrossRef]
65. Gohoho, H.D.; Noby, H.; Hayashi, J.; El-shazlyShazly, A.H. Various acids functionalized polyaniline-peanut shell activated carbon composites for dye removal. *J. Mater. Cycles Waste Manag.* **2022**, *24*, 1508–1523. [CrossRef]
66. Lahreche, S.; Moulefera, I.; El Kebir, A.; Sabantina, L.; Kaid, M.; Benyoucef, A. Application of activated carbon adsorbents prepared from prickly pear fruit seeds and a conductive polymer matrix to remove congo red from aqueous solutions. *Fibers* **2022**, *10*, 7. [CrossRef]
67. Meena, P.L.; Saini, J.K.; Surela, A.K.; Poswal, K.; Chhachhia, L.K. Fabrication of polyaniline-coated porous and fibrous nanocomposite with granular morphology using tea waste carbon for effective removal of rhodamine B dye from water samples. *Biomass Convers. Biorefinery* **2022**, 1–20. [CrossRef]
68. Li, R.; Li, T.; Wan, Y.; Zhang, X.; Liu, X.; Li, R.; Pu, H.; Gao, T.; Wang, X.; Zhou, Q. Efficient decolorization of azo dye wastewater with polyaniline/graphene modified anode in microbial electrochemical systems. *J. Hazard. Mater.* **2021**, *421*, 126740. [CrossRef]
69. Khan, M.A.; Govindasamy, R.; Ahmad, A.; Siddiqui, M.; Alshareef, S.; Hakami, A.; Rafatullah, M. Carbon based polymeric nanocomposites for dye adsorption: Synthesis, characterization, and application. *Polymers* **2021**, *13*, 419. [CrossRef]
70. Razzaq, S.; Akhtar, M.; Zulfiqar, S.; Zafar, S.; Shakir, I.; Agboola, P.O.; Haider, S.; Warsi, M.F. Adsorption removal of Congo red onto L-cysteine/rGO/PANI nanocomposite: Equilibrium, kinetics and thermodynamic studies. *J. Taibah Univ. Sci.* **2021**, *15*, 50–62. [CrossRef]
71. Katowah, D.F.; Saleh, S.M.; Alqarni, S.A.; Ali, R.; Mohammed, G.I.; Hussein, M.A. Network structure-based decorated CPA@CuO hybrid nanocomposite for methyl orange environmental remediation. *Sci. Rep.* **2021**, *11*, 1–21. [CrossRef]
72. Singh, A.R.; Dhumal, P.S.; Bhakare, M.A.; Lokhande, K.D.; Bondarde, M.P.; Some, S. In-situ synthesis of metal oxide and polymer decorated activated carbon-based photocatalyst for organic pollutants degradation. *Sep. Purif. Technol.* **2022**, *286*, 120380. [CrossRef]
73. Liu, Y.; Wu, F.; Tian, X.; Hu, X.; Liu, Y.; Zhao, X.; Qu, R.; Ji, C.; Niu, Y. Polyaniline dispersed by Kevlar fiber for uptake of organic dye. *Pigment Resin Technol.* **2020**, *50*, 346–355. [CrossRef]
74. Liu, M.-L.; Li, L.; Sun, Y.-X.; Fu, Z.-J.; Cao, X.-L.; Sun, S.-P. Scalable conductive polymer membranes for ultrafast organic pollutants removal. *J. Membr. Sci.* **2021**, *617*, 118644. [CrossRef]
75. Jahan, K.; Tyeb, S.; Kumar, N.; Verma, V. Bacterial cellulose-polyaniline porous mat for removal pf methyl orange and bacterial pathogens from potable water. *J. Polym. Environ.* **2021**, *29*, 1257–1270. [CrossRef]
76. Mansor, E.S.; Ali, H.; Abdel-Karim, A. Efficient and reusable polyethylene oxide/polyaniline composite membrane for dye adsorption and filtration. *Colloids Interface Sci. Commun.* **2020**, *39*, 100314. [CrossRef]
77. Mendieta-Rodríguez, L.S.; González-Rodríguez, L.M.; Alcaraz-Espinoza, J.J.; Chávez-Guajardo, A.E.; Medina-Llamas, J.C. Synthesis and characterization of a polyurethane-polyaniline macroporous foam material for methyl orange removal in aqueous media. *Mater. Today Commun.* **2021**, *26*, 102–155. [CrossRef]
78. Bagheri, N.; Lakouraj, M.M.; Hasantabar, V.; Mohseni, M. Biodegradable macro-porous CMC-polyaniline hydrogel: Synthesis, characterization and study of microbial elimination and sorption capacity of dyes from waste water. *J. Hazard. Mater.* **2021**, *403*, 123631. [CrossRef]

79. Alam, J.; Shukla, A.K.; Ansari, M.A.; Ali, F.A.A.; Alhoshan, M. Dye separation and antibacterial activities of polyaniline thin film-coated poly(phenyl sulfone) membranes. *Membranes* **2021**, *11*, 25. [CrossRef]
80. Mahi, O.; Khaldi, K.; Belardja, M.S.; Belmokhtar, A.; Benyoucef, A. Development of a New Hybrid Adsorbent from Opuntia Ficus Indica NaOH-Activated with PANI-Reinforced and Its Potential Use in Orange-G Dye Removal. *J. Inorg. Organomet. Polym. Mater.* **2021**, *31*, 2095–2104. [CrossRef]
81. Imgharn, A.; Ighnih, H.; Hsini, A.; Naciri, Y.; Laabd, M.; Kabli, H.; Elamine, M.; Lakhmiri, R.; Souhail, B.; Albourine, A. Synthesis and characterization of polyaniline-based biocomposites for effective removal of Orange G dye adsorption in dynamic regime. *Chem. Phys. Lett.* **2021**, *778*, 138811. [CrossRef]
82. Mashkoor, F.; Nasar, A. Facile synthesis of polypyrrole decorated chitosan-based magsorbent: Characterizations, performance, and applications in removing cationic and anionic dyes from aqueous medium. *Int. J. Biol. Macromol.* **2020**, *161*, 88–100. [CrossRef] [PubMed]
83. Li, H.; Zhang, J.; Zhu, L.; Liu, H.; Yu, S.; Xue, J.; Zhu, X.; Xue, Q. Reusable membrane with multifunctional skin layer for effective removal of insoluble emulsified oils and soluble dyes. *J. Hazard. Mater.* **2021**, *415*, 125677. [CrossRef] [PubMed]
84. Nawaz, H.; Umar, M.; Nawaz, I.; Zia, Q.; Tabassum, M.; Razzaq, H.; Gong, H.; Zhao, X.; Liu, X. Photodegradation of textile pollutants by nanocomposite membranes of polyvinylidene fluoride integrated with polyaniline–titanium dioxide nanotubes. *Chem. Eng. J.* **2021**, *419*, 129542. [CrossRef]
85. Nawaz, H.; Umar, M.; Nawaz, I.; Ullah, A.; Khawar, M.T.; Nikiel, M.; Razzaq, H.; Siddiq, M.; Liu, X. Hybrid PVDF/PANI membrane for removal of dyes from textile wastewater. *Adv. Eng. Mater.* **2021**, *24*, 2100719. [CrossRef]
86. Imgharn, A.; Aarab, N.; Hsini, A.; Naciri, Y.; Elhoudi, M.; Haki, M.A.; Laabd, M.; Lakhmiri, R.; Albourine, A. Application of calcium alginate-PANI@sawdust wood hydrogel bio-beads for the removal of orange G dye from aqueous solution. *Environ. Sci. Pollut. Res.* **2022**, *29*, 60259–60268. [CrossRef]
87. Maruthapandi, M.; Saravanan, A.; Manohar, P.; Luong, J.; Gedanken, A. Photocatalytic degradation of organic dyes and antimicrobial activities by polyaniline–nitrogen-doped carbon dot nanocomposite. *Nanomaterials* **2021**, *11*, 1128. [CrossRef]
88. Yuan, X.; Kobylanski, M.P.; Cui, Z.; Li, J.; Beaunier, P.; Dragoe, D.; Colbeau-Justin, C.; Zaleska-Medynska, A.; Remita, H. Highly active composite TiO_2-polypyrrole nanostructures for water and air depollution under visible light irradiation. *J. Environ. Chem. Eng.* **2020**, *8*, 104178. [CrossRef]
89. Demir, M.; Taymaz, B.H.; Sarıbel, M.; Kamış, H. Photocatalytic Degradation of Organic Dyes with Magnetically Separable PANI/Fe_3O_4 Composite under Both UV and Visible-light Irradiation. *ChemistrySelect* **2022**, *7*, e202103787. [CrossRef]
90. Riyat, R.I.; Salam, A.; Molla, T.H.; Islam, S.; Bashar, A.; Chandra, D.; Ahsan, S.; Roy, D. Magnetically recyclable core–shell structured $Co_{0.5}Zn_{0.5}Fe_2O_4$@polyaniline nanocomposite: High stability and rapid photocatalytic degradation of commercial azo dyes and industrial effluents. *React. Kinet. Mech. Catal.* **2022**, *135*, 1077–1098. [CrossRef]
91. Liu, G.; Wang, Y.; Xue, Q.; Wen, Y.; Hong, X.; Ullah, K. TiO_2/Cu-MOF/PPy composite as a novel photocatalyst for decomposition of organic dyes. *J. Mater. Sci. Mater. Electron.* **2021**, *32*, 4097–4109. [CrossRef]
92. Mittal, H.; Khanuja, M. Hydrothermal in-situ synthesis of $MoSe_2$-polypyrrole nanocomposite for efficient photocatalytic degradation of dyes under dark and visible light irradiation. *Sep. Purif. Technol.* **2020**, *254*, 117508. [CrossRef]
93. Taymaz, B.H.; Kamiş, H.; Yoldaş, O. Photocatalytic degradation of malachite green dye using zero valent iron doped polypyrrole. *Environ. Eng. Res.* **2021**, *27*, 200638. [CrossRef]
94. Liu, T.; Wang, Z.; Wang, X.; Yang, G.; Liu, Y. Adsorption-photocatalysis performance of polyaniline/dicarboxyl acid cellulose@graphene oxide for dye removal. *Int. J. Biol. Macromol.* **2021**, *182*, 492–501. [CrossRef] [PubMed]
95. Mansor, E.S.; Geioushy, R.A.; Fouad, O.A. PANI/BiOCl nanocomposite induced efficient visible-light photocatalytic activity. *J. Mater. Sci. Mater. Electron.* **2021**, *32*, 1992–2000. [CrossRef]
96. Sharma, S.; Kumar, D.; Khare, N. Hierarchical PANI/CdS nanoarchitecture system for visible light included photocatalytic dye degradation and photoelectrochemical water splitting. *Polymer* **2021**, *231*, 124117. [CrossRef]
97. Qutub, N.; Singh, P.; Sabir, S.; Umar, K.; Sagadevan, S.; Oh, W.-C. Synthesis of polyaniline supported CdS/CdS-ZnS/CdS-TiO_2 nanocomposite for efficient photocatalytic applications. *Nanomaterials* **2022**, *12*, 1355. [CrossRef]
98. Kumar, A.; Mittal, H.; Nagar, R.; Khanuja, M. The synergistic effect of acid-etched *g*-C_3N_4 nanosheets and polyaniline nanofibers for the adsorption and photocatalytic degradation of textile dyes: A study of charge transfer mechanism and intermediate products. *Mater. Adv.* **2022**, *3*, 5325–5336. [CrossRef]
99. Ardani, M.R.; Pang, A.L.; Pal, U.; Zheng, R.; Arsad, A.; Hamzah, A.A.; Ahmadipour, M. Ultrasonic-assisted polyaniline-multiwall carbon nanotube photocatalyst for efficient photodegradation of organic pollutants. *J. Water Process Eng.* **2022**, *46*, 102557. [CrossRef]
100. Bhaumik, M.; Maity, A.; Brink, H.G. Metallic nickel nanoparticles supported polyaniline nanotubes as heterogeneous Fenton-like catalyst for the degradation of brilliant green dye in aqueous solution. *J. Colloid Interface Sci.* **2021**, *611*, 408–420. [CrossRef]
101. Fenniche, F.; Henni, A.; Khane, Y.; Aouf, D.; Harfouche, N.; Bensalem, S.; Zerrouki, D.; Belkhalfa, H. Electrochemical synthesis of reduced graphene oxide–wrapped polyaniline nanorods for improved photocatalytic and antibacterial activities. *J. Inorg. Organomet. Polym. Mater.* **2022**, *32*, 1011–1025. [CrossRef]
102. Kumar, H.; Luthra, M.; Punia, M.; Singh, D. Ag_2O@PANI nanocomposites for advanced functional applications: A sustainable experimental and theoretical approach. *Colloids Surf. A Physicochem. Eng. Asp.* **2022**, *640*, 128464. [CrossRef]

103. Sayed, M.A.; Ahmed, M.; El-Shahat, M.; El-Sewify, I.M. Mesoporous polyaniline/SnO_2 nanospheres for enhanced photocatalytic degradation of bio-staining fluorescent dye from an aqueous environment. *Inorg. Chem. Commun.* **2022**, *139*, 109326. [CrossRef]
104. Rahman, K.H.; Kar, A.K. Effect of band gap variation and sensitization process of polyaniline (PANI)-TiO_2 p-n heterojunction photocatalysts on the enhancement of photocatalytic degradation of toxic methylene blue with UV irradiation. *J. Environ. Chem. Eng.* **2020**, *8*, 104181. [CrossRef]
105. Aminuddin, N.; Nawi, M.; Bahrudin, N.; Jawad, A. Iron ion assisted photocatalytic-adsorptive removal of acid orange 52 by immobilized TiO_2/polyaniline bilayer photocatalyst. *Appl. Surf. Sci. Adv.* **2021**, *6*, 100180. [CrossRef]
106. Aminuddin, N.; Nawi, M.; Bahrudin, N. Enhancing the optical properties of immobilized TiO_2/polyaniline bilayer photocatalyst for methyl orange decolorization. *React. Funct. Polym.* **2022**, *174*, 105248. [CrossRef]
107. Naciri, Y.; Hsini, A.; Bouziani, A.; Tanji, K.; El Ibrahimi, B.; Ghazzal, M.; Bakiz, B.; Albourine, A.; Benlhachemi, A.; Navío, J.; et al. Z-scheme WO_3/PANI heterojunctions with enhanced photocatalytic activity under visible light: A depth experimental and DFT studies. *Chemosphere* **2021**, *292*, 133468. [CrossRef]
108. Hamdy, M.S.; Abd-Rabboh, H.S.; Benaissa, M.; Al-Metwaly, M.G.; Galal, A.; Ahmed, M. Fabrication of novel polyaniline/ZnO heterojunction for exceptional photocatalytic hydrogen production and degradation of fluorescein dye through direct Z-scheme mechanism. *Opt. Mater.* **2021**, *117*, 111198. [CrossRef]
109. Belabed, C.; Tab, A.; Moulai, F.; Černohorský, O.; Boudiaf, S.; Benrekaa, N.; Grym, J.; Trari, M. ZnO nanorods-PANI heterojunction dielectric, electrochemical properties, and photodegradation study of organic pollutant under solar light. *Int. J. Hydrogen Energy* **2021**, *46*, 20893–20904. [CrossRef]
110. Yadav, A.; Kumar, H. Polyaniline Plastic Nanocomposite as Multi-Functional Nanomaterial. *ChemistrySelect* **2022**, *7*, 202201475. [CrossRef]
111. Kumaresan, A.; Arun, A.; Kalpana, V.; Vinupritha, P.; Sundaravadivel, E. Polymer-supported $NiWO_4$ nanocomposites for visible light degradation of toxic dyes. *J. Mater. Sci. Mater. Electron.* **2022**, *33*, 9660–9668. [CrossRef]
112. Ding, W.P.; Li, J.D.; Chen, S.W.; Li, X.G.; Wang, Q.; He, A.Y.; Yin, J.Z. Attapulgite/*g*-C_3N_4-Pt/polyaniline composites: Preparation and visible light photocatalytic properties. *Chin. J. Inorg. Chem.* **2022**, *38*, 253–260. [CrossRef]
113. Chen, Y.; Wang, T.; Pan, J.; Wang, M.; Chen, A.; Chen, Y. Fabrication, characterization and photocatalytic degradation activity of PS/PANI/CeO_2 tri-layer nanostructured hybrids. *Bull. Mater. Sci.* **2022**, *45*, 1–9. [CrossRef]
114. Shashikala, B.S.; Al-Gunaid, M.Q.A.; Somesh, T.E.; Anasuya, S.J. Core–shell synergistic effect of (PANI-$NaBiO_2$) incorporated polycarbonate films to photodegradation of MG dye and photovoltaic activity. *Polym. Bull.* **2022**, *79*, 7531–7554. [CrossRef]
115. Palliyalil, S.; Chola, R.K.V.; Vigneshwaran, S.; Poovathumkuzhi, N.C.; Chelaveettil, B.M.; Meenakshi, S. Ternary system of TiO_2 confined chitosan–polyaniline heterostructure photocatalyst for the degradation of anionic and cationic dyes. *Environ. Technol. Innov.* **2022**, *28*, 102586. [CrossRef]
116. Liu, S.; Hu, J.; Wu, D.; Zeng, H.; Zhou, T.; Yang, M.; Feng, Q. Preparation of spunlaced viscose/PANI-ZnO/GO fiber membrane and its performance of photocatalytic decolorization. *J. Ind. Text.* **2022**, *51*, 7359S–7373S. [CrossRef]
117. Jumat, N.A.; Khor, S.-H.; Basirun, W.J.; Juan, J.-C.; Phang, S.-W. Highly Visible Light Active Ternary Polyaniline-TiO_2-Fe_3O_4 Nanotube/Nanorod for Photodegradation of Reactive Black 5 Dyes. *J. Inorg. Organomet. Polym. Mater.* **2021**, *31*, 2168–2181. [CrossRef]
118. Zare, N.; Kojoori, R.K.; Abdolmohammadi, S.; Sadegh-Samiei, S. Ultrasonic-assisted synthesis of highly effective visible light Fe_3O_4/ZnO/PANI nanocomposite: Thoroughly kinetics and thermodynamic investigations on the Congo red dye decomposition. *J. Mol. Struct.* **2021**, *1250*, 131903. [CrossRef]
119. Liu, S.; Jiang, X.; Waterhouse, G.I.; Zhang, Z.-M.; Yu, L.-M. Protonated graphitic carbon nitride/polypyrrole/reduced graphene oxide composites as efficient visible light driven photocatalysts for dye degradation and *E. coli* disinfection. *J. Alloy. Compd.* **2021**, *873*, 159750. [CrossRef]
120. Bahadoran, A.; Baghbadorani, N.B.; De Lile, J.R.; Masudy-Panah, S.; Sadeghi, B.; Li, J.; Ramakrishna, S.; Liu, Q.; Janani, B.J.; Fakhri, A. Ag doped Sn_3O_4 nanostructure and immobilized on hyperbranched polypyrrole for visible light sensitized photocatalytic, antibacterial agent and microbial detection process. *J. Photochem. Photobiol. B Biol.* **2022**, *228*, 112393. [CrossRef]
121. Zhang, T.; Guo, R.; Ying, G.; Lu, Z.; Peng, C.; Shen, M.; Zhang, J. Absolute film separation of dyes/salts and emulsions with a superhigh water permeance through graded nanofluidic channels. *Mater. Horizons* **2022**, *9*, 1536–1542. [CrossRef] [PubMed]
122. Shi, X.-Y.; Gao, M.-H.; Hu, W.-W.; Luo, D.; Hu, S.-Z.; Huang, T.; Zhang, N.; Wang, Y. Largely enhanced adsorption performance and stability of MXene through in-situ depositing polypyrrole nanoparticles. *Sep. Purif. Technol.* **2022**, *287*, 120596. [CrossRef]
123. Yan, Y.Y.; Zhou, P.Z.; Zhang, S.; Yin, X.Y.; Zeng, X.J.; Pi, P.H.; Nong, Y.J.; Wen, X.F. Facile preparation of ultralong polypyrrole nanowires-coated membrane for switchable emulsions separation and dyes adsorption. *J. Water Process Eng.* **2022**, *49*, 102942. [CrossRef]
124. Lai, X.; Wang, C.; Wang, L.; Xiao, C. A novel PPTA/PPy composite organic solvent nanofiltration (OSN) membrane prepared by chemical vapor deposition for organic dye wastewater treatment. *J. Water Process Eng.* **2022**, *45*, 102533. [CrossRef]
125. Zhang, D.; Yang, J.; Qiao, G.; Wang, J.; Li, H. Facile two-step synthesis of nanofiber polyaniline/graphene/cuprous oxide composite with enhanced photocatalytic performance. *Appl. Nanosci.* **2021**, *11*, 983–993. [CrossRef]
126. Attia, N.F.; Shaltout, S.M.; Salem, I.A.; Zaki, A.B.; El-Sadek, M.H.; Salem, M.A. Sustainable and smart hybrid nanoporous adsorbent derived biomass as efficient adsorbent for cleaning of wastewater from Alizarin Red dye. *Biomass Convers. Biorefinery* **2022**, 1–16. [CrossRef]

127. Wang, Y.; Chen, R.; Dai, Z.; Yu, Q.; Miao, Y.; Xu, R. Facile preparation of a polypyrrole modified Chinese yam peel-based adsorbent: Characterization, performance, and application in removal of Congo red dye. *RSC Adv.* **2022**, *12*, 9424–9434. [CrossRef]
128. Huang, F.; Tian, X.; Wei, W.; Xu, X.; Li, J.; Guo, Y.; Zhou, Z. Wheat straw-core hydrogel spheres with polypyrrole nanotubes for the removal of organic dyes. *J. Clean. Prod.* **2022**, *344*, 131100. [CrossRef]
129. Heybet, E.N.; Ugraskan, V.; Isik, B.; Yazici, O. Adsorption of methylene blue dye on sodium alginate/polypyrrole nanotube composites. *Int. J. Biol. Macromol.* **2021**, *193*, 88–99. [CrossRef]
130. Maqbool, M.; Sadaf, S.; Bhatti, H.N.; Rehmat, S.; Kausar, A.; Alissa, S.A.; Iqbal, M. Sodium alginate and polypyrrole composites with algal dead biomass for the adsorption of Congo red dye: Kinetics, thermodynamics and desorption studies. *Surfaces Interfaces* **2021**, *25*, 101183. [CrossRef]
131. Qi, F.-F.; Ma, T.-Y.; Liu, Y.; Fan, Y.-M.; Li, J.-Q.; Yu, Y.; Chu, L.-L. 3D superhydrophilic polypyrrole nanofiber mat for highly efficient adsorption of anionic azo dyes. *Microchem. J.* **2020**, *159*, 105389. [CrossRef]
132. Yu, Y.; Su, J.; Liu, J.; Li, W. Magnetic poly(glycidyl methacrylate) microspheres with grafted polypyrrole chains for the high-capacity adsorption of Congo red dye from aqueous solutions. *Coatings* **2022**, *12*, 168. [CrossRef]
133. Li, Y.; Yan, S.; Jia, X.; Wu, J.; Yang, J.; Zhao, C.; Wang, S.; Song, H.; Yang, X. Uncovering the origin of full-spectrum visible-light-responsive polypyrrole supramolecular photocatalysts. *Appl. Catal. B: Environ.* **2021**, *287*, 119926. [CrossRef]
134. Taymaz, B.H.; Taş, R.; Kamış, H.; Can, M. Photocatalytic activity of polyaniline and neutral polyaniline for degradation of methylene blue and malachite green dyes under UV Light. *Polym. Bull.* **2021**, *78*, 2849–2865. [CrossRef]
135. Hussain, D.; Siddiqui, M.F.; Shirazi, Z.; Alam Khan, T. Evaluation of adsorptive and photocatalytic degradation properties of $FeWO_4$/polypyrrole nanocomposite for rose bengal and alizarin red S from liquid phase: Modeling of adsorption isotherms and kinetics data. *Environ. Prog. Sustain. Energy* **2022**, *41*, 13822. [CrossRef]
136. Pang, A.L.; Arsad, A.; Ahmadipour, M.; Hamzah, A.A.; Zaini, M.A.A.; Mohsin, R. High efficient degradation of organic dyes by polypyrrole-multiwall carbon nanotubes nanocomposites. *Polym. Adv. Technol.* **2022**, *33*, 1402–1411. [CrossRef]
137. Punnakkal, V.S.; Jos, B.; Anila, E.I. Polypyrrole-silver nanocomposite for enhanced photocatalytic degradation of methylene blue under sunlight irradiation. *Mater. Lett.* **2021**, *298*, 130014. [CrossRef]
138. Koysuren, H.N.; Koysuren, O. Improving UV light photocatalytic activity of WO_3 by doping with boron and compounding with polypyrrole. *Biointerface Res. Appl. Chem.* **2022**, *13*, 86. [CrossRef]
139. Capilli, G.; Sartori, D.R.; Gonzalez, M.C.; Laurenti, E.; Minero, C.; Calza, P. Non-purified commercial multiwalled carbon nanotubes supported on electrospun polyacrylonitrile@polypyrrole nanofibers as photocatalysts for water decontamination. *RSC Adv.* **2021**, *11*, 9911–9920. [CrossRef]
140. Yu, H.; He, Y.; Li, H.; Li, Z.; Ren, B.; Chen, G.; Hu, X.; Tang, T.; Cheng, Y.; Ou, J.Z. Core-shell PPy@TiO_2 enable GO membranes with controllable and stable dye desalination properties. *Desalination* **2022**, *526*, 115523. [CrossRef]
141. Elkady, M.; Hassan, H. Photocatalytic Degradation of malachite green dye from aqueous solution using environmentally compatible Ag/ZnO polymeric nanofibers. *Polymers* **2021**, *13*, 2033. [CrossRef] [PubMed]
142. Habtamu, F.; Berhanu, S.; Mender, T. Polyaniline supported Ag-doped ZnO nanocomposite: Synthesis, characterization, and kinetics study for photocatalytic degradation of malachite green. *J. Chem.* **2021**, *2021*, 2451836. [CrossRef]
143. Biju, R.; Ravikumar, R.; Thomas, C.; Indulal, C.R. Enhanced photocatalytic degradation of Metanil Yellow dye using polypyrrole-based copper oxide–zinc oxide nanocomposites under visible light. *J. Nanoparticle Res.* **2022**, *24*, 1–16. [CrossRef]
144. Mohamed, H.G.; Aboud, A.A.; El-Salam, H.A. Synthesis and characterization of chitosan/polyacrylamide hydrogel grafted poly(*N*-methylaniline) for methyl red removal. *Int. J. Biol. Macromol.* **2021**, *187*, 240–250. [CrossRef] [PubMed]
145. Stejskal, J. Polymers of phenylenediamines. *Prog. Polym. Sci.* **2015**, *41*, 1–31. [CrossRef]
146. Ma, G.; Zhao, S.; Wang, Y.; Wang, Z.; Wang, J. Conjugated polyaniline derivative membranes enable ultrafast nanofiltration and organic-solvent nanofiltration. *J. Membr. Sci.* **2022**, *645*, 120241. [CrossRef]
147. Trchová, M.; Konyushenko, E.N.; Stejskal, J.; Kovářová, J.; Ćirić-Marjanović, G. The conversion of polyaniline nanotubes to nitrogen-containing carbon nanotubes and their comparison with multi-walled carbon nanotubes. *Polym. Degrad. Stab.* **2009**, *94*, 929–938. [CrossRef]
148. Cheng, H.; Zhang, W.; Liu, X.; Tang, T.; Xiong, J. Fabrication of Titanium Dioxide/Carbon Fiber (TiO_2/CF) Composites for Removal of Methylene Blue (MB) from Aqueous Solution with Enhanced Photocatalytic Activity. *J. Chem.* **2021**, *2021*, 9986158. [CrossRef]
149. Munusamy, S.; Sivaranjan, K.; Sabhapathy, P.; Narayanan, V.; Mohammad, F.; Sagadevan, S. Enhanced electrochemical and photocatalytic activity of g-C_3N_4-PANI-PPy nanohybrids. *Synth. Met.* **2020**, *272*, 116669. [CrossRef]
150. Mahmud, H.N.M.E.; Kamal, S.J.; Mohamad, N.; Sharma, A.K.; Saharan, P.; Santos, J.H.; Zakaria, S.N.A. Nanoconducting polymer: An effective adsorbent for dyes. *Chem. Pap.* **2021**, *75*, 5173–5185. [CrossRef]
151. Stejskal, J.; Kohl, M.; Trchová, M.; Kolská, Z.; Pekárek, M.; Křivka, I.; Prokeš, J. Conversion of conducting polypyrrole nanostructures to nitrogen containing carbons and its impact on the adsorption of organic dye. *Mater. Adv.* **2021**, *2*, 706–717. [CrossRef]
152. Stejskal, J.; Trchová, M.; Lapčák, L.; Kolská, Z.; Kohl, M.; Pekárek, M.; Prokeš, J. Comparison of carbonized and activated polypyrrole globules, nanofibers, and nanotubes as conducting nanomaterials and adsorbents of organic dye. *Carbon Trends* **2021**, *4*, 100068. [CrossRef]
153. Stejskal, J. Conducting polymers are not just conducting: A perspective for emerging technology. *Polym. Int.* **2020**, *69*, 662–664. [CrossRef]